Biochemistry and Biophysics Reports 7 (2016) 328–337

Contents lists available at ScienceDirect

Biochemistry and Biophysics Reports

journal homepage: www.elsevier.com/locate/bbrep

Cathepsin-L and transglutaminase dependent processing of ps20: A novel mechanism for ps20 regulation via ECM cross-linking

Oliver J. Hickman [a], Prokar Dasgupta [b], Christine Galustian [b], Richard A. Smith [b,*,1], Annapurna Vyakarnam [a,c,**,1]

[a] Department of Infectious Diseases, King's College London, United Kingdom
[b] Division of Transplantation Immunology and Mucosal Biology, King's College London, United Kingdom
[c] Centre for Infectious Disease Research, Indian Institute of Science, Bangalore 560012, India

ARTICLE INFO

Article history:
Received 11 August 2015
Received in revised form
16 May 2016
Accepted 13 June 2016
Available online 15 June 2016

Keywords:
Prostate cancer
Transglutaminase
Cathepsin
Ps20
Whey-four-disulphide core
Glycosaminoglycan

ABSTRACT

Whey-acidic-protein (WAP) four-disulphide core (WFDC) proteins have important roles in the regulation of innate immunity, anti-microbial function, and the inhibition of inflammatory proteases at mucosal surfaces. It was recently demonstrated that the WFDC protein, prostate stromal 20 (ps20), encoded by the WFDC1 gene, is a potent growth inhibitory factor, and shares with other WFDC proteins the ability to modulate wound healing processes and immune responses to viral infections. However, ps20 remains relatively uncharacterised at the protein level.

Using a panel of ps20 antibodies for western-blotting (WB), ELISA and immunoaffinity purification, we isolated, biochemically characterised and tested ps20 preparations for three biological properties: (i) interactions with glycosaminoglycans (GAG) (ii) inhibition of cell proliferation, and (iii) transglutaminase2 (TG2) mediated crosslinking of ps20 to fibronectin, a process implicated in wound healing. We show herein that ps20 preparations contain multiple molecular forms including full-length ps20 (resolving at $\approx$ 27 kDa), an exon 3 truncated form ($\approx$ 22 kDa) that lacks aa113–140, and variable amounts of a putatively cleaved lower MW ($\approx$ 15–17 kDa) species. Untagged purified ps20 preparations containing a mixture of these forms are biologically active in significantly suppressing prostate cell proliferation. We show that one mechanism by which lower LMW forms of ps20 arise is through cathepsin L (CL) cleavage, and confirm that CL cleaves ps20 at the C-terminus, but this does not inhibit its growth inhibitory function. However, CL cleavage abrogated the interaction between ps20 and solid-phase fibronectin.

Therefore, we demonstrate for the first time that LMW forms of ps20 that lack a C-terminal immunogenic epitope can arise through CL cleavage and this cleavage impairs multimerisation and potential capacity to cross-link to ECM, but not the capacity of ps20 to inhibit cell proliferation. We propose that ps20 like other WFDC proteins can become associated with GAGs and the ECM. Furthermore, we suggest post-translational processing and cleavage of ps20 is required to generate functional protein species, and TG2 mediated crosslinking and CL cleavage form components of a ps20 regulatory apparatus.

1. Introduction

The WFDC family of proteins are potent modulators of inflammation defined by presence of a tightly coiled globular WAP-four-disulphide-core domain. Members possess pleiotropic roles in the inhibition of inflammatory proteases, abrogation of microbial growth, and the ability to regulate the responses to viral infections [1,2]. ps20 is a WFDC family member for which no protease inhibitory function has yet been elucidated, but nonetheless possesses potent immune regulatory functions including the modulation of cell and molecular responses to viral infection and wounding [2–4]. Other data show ps20 to be a physiologically pleiotropic protein able to regulate numerous downstream host

Abbreviations: WFDC1, whey acidic protein four disulphide core 1; GAG, glycosaminoglycan; ps20, prostate stromal 20; rps20, recombinant ps20; FL, full length; TR, truncated; MW, molecular weight; HMW, high molecular weight; LMW, low molecular weight; ECM, extracellular matrix; CL, cathepsin L; CM, conditioned media; CV, column volume; WB, western blot

* Correspondence to: King's College London, Guys Hospital, Great Maze Pond, London SE1 9RT, United Kingdom.
** Corresponding author at: Department of Infectious Diseases, King's College London, United Kingdom. nn Correspondence to: King's College London.
E-mail addresses: richard.a.smith@kcl.ac.uk (R.A. Smith), anna.vyakarnam@kcl.ac.uk (A. Vyakarnam).
[1] Equal Joint Authors.

http://dx.doi.org/10.1016/j.bbrep.2016.06.010

factors such as ICAM-1 and IL-8 with effects on processes as diverse as tumourigenesis and HIV infectivity [3,5]. Unique within the WFDC family, ps20 is a potent inhibitor of cellular proliferation and has putative role in regulating replicative senescence [6–9]. In keeping with this notion WFDC1/ps20 is downregulated in diverse tumour types including prostate cancer [9–12].

WFDC1 is expressed in two isoforms at the mRNA level, one containing a full length 660 mRNA coding sequence formed of 6 exons, and a truncated form containing a 576 bp coding sequence in which exon 3 is absent. Both were originally observed in prostate cancer cell lines and patient samples [6]. We have recently published evidence that both forms are transcribed and expressed at the protein level [13]. Despite the importance of WFDC family proteins in numerous disease processes, their biochemistry is poorly understood, including their means of interacting with cells and signalling. Although all WFDC factors are secreted, all members including ps20 lack known cell surface receptors, or the ability to signal by any known mechanism, despite showing significant cell-intrinsic functionality [14]. While binding to a number of cell surface proteins has been observed for SLPI, none of these has been linked to specific cellular functions [2]. Interestingly however, both SLPI and elafin are known to interact with glycosaminoglycans (GAGs) [15,16]. These sulphated disaccharide chains are ubiquitous at the surface of cells and in the ECM where they sequester soluble proteins and mediate ligand-receptor interactions [17,18]. It has been proposed that endocytic and macropinocytotic uptake of proteins may involve proteoglycans [19,20], which may be pertinent to WFDC protein function given that labelled SLPI has been shown to enter cells, locate to the nucleus, and function by binding to NFκB regulatory elements [21,22].

In addition to binding GAGs, SLPI and elafin interact with TG2, a calcium dependent enzyme responsible for crosslinking of protein multimers [23]. Furthermore, both SLPI and elafin undergo TG2 mediated crosslinking to ECM components fibronectin and elastin [24,25] tethering them within the ECM from where they can perform their protease inhibition and immune-modulatory functions. WFDC proteins are also susceptible to cleavage by cathepsins; elafin is cleaved from its precursor trappin-2 by cathepsins-L and -K [26] while SLPI is inactivated by cleavage by cathepsins-B, L and S [27]. TG2 crosslinking and cathepsin cleavage are therefore potential mechanisms for regulating WFDC protein function and may be pertinent to ps20 function.

Few papers have investigated the use of soluble ps20, despite its therapeutic potential as a potent inhibitor of tumour growth and immune regulatory factor. Herein we demonstrate a novel method for the purification of ps20, and demonstrate ps20-GAG interactions. Furthermore we demonstrate that ps20 cleavage by CL does not abrogate ps20 growth inhibitory function. Lastly, we show that ps20 interacts with both TG2 and cathepsins, and propose a role for these processes in regulation of ps20 bioavailability within the ECM.

2. Materials and methods

2.1. Cell lines

PC-3, and WPMY-1 cells were purchased from the ATCC (Manassas, Virginia). HeLa and 293T cells were a kind gift of Professor Mike Malim (KCL, dept. infectious Diseases). 293F cells, a suspension-culture adapted variant of HEK 293T, were purchased from Life Technologies. Cell lines were routinely cultured in DMEM (WPMY-1, 293T) or RPMI (HeLa, PC-3) with 10% FCS, 2mM L-glutamine and antibiotics at 37 °C with 5% CO_2 in 75 cm^2 flasks. 293F were cultured in FreeStyle™ 293 expression medium in conical flasks. All media and serum was purchased from Gibco (Life Technologies).

2.2. Antibodies

Ps20 antibodies: Mouse monoclonal 1G7 was generated as previously described [6]. C-terminal and N-terminal polyclonal abs specific to ps20 were generated by Eurogentech (Southampton, UK) by inoculation of rabbits with peptides AEEAGAPGGPRQPRA and KNVAEPGRGQQKHFQ respectively (Supplementary Fig. 1). Purification was by affinity chromatography to the immunising peptide. Where these antibodies are used in western blotting (WB) they are labelled C-term and N-term respectively. Antibody to V5-tag was from Sigma. Antibody to β-actin was from Santa Cruz Biotechnology. HRP-conjugated goat anti-rabbit and rabbit anti-goat used for WB were from thermo-scientific.

2.3. Cloning and verification of full-length and truncated ps20

WFDC1 mRNA transcripts were amplified from HeLa-lysate with specific primers: 5′-GGGAGGAAATGCCTTTAACC-3′ and 5′-TGCTTGCCGTTGCTTTACTG-3′. EcoR1 and Xho1 sites were added through amplification with Taq polymerase (New England Biolabs) using the primers fwd 5′-ATATATACTCGAGGCATGCCTTTCCGGC-3′ and rev 5′-ATATATGAATTCGCTTACTGAAAGTGCTTCTG-3′ and the resulting products ligated into the MIGR1-EGFP plasmid (a kind gift of Professor Mike Malim). Plasmids were verified by sequencing (MWG eurofins).

2.4. Purification of ps20 for functional studies

Four sources of ps20 were used as described below. For functional studies, we generated sufficient quantities of both native ps20 purified from HeLa cell conditioned media (described in Section 2.4.1 below) as well as recombinant (r) ps20 (described in Section 2.4.2 below). For additional biochemical analyses, we generated recombinant full length ($rps20^{FL}$), and recombinant truncated ps20 ($rps20^{TR}$), representing ps20 molecule expressed from the full length WFDC1 coding sequence, or an isoform in which the whole of exon 3 has been removed (described in Section 2.4.3 below). Lastly, in some experiments we used a V5-His tagged recombinant ps20 ($rps20^{V5}$) (described in Section 2.4.4 below).

2.4.1. $ps20^{HeLa}$

Purification of native ps20 secreted by HeLa cells was performed by BIOSERV Ltd (Sheffield, UK). Briefly, HeLa cells were cultured in HyClone™ SFM4CHO™ Media (GE healthcare) in roller bottles for 72 h. Conditioned media (CM) was concentrated 10 × using a vivaflow 200, 5 kDa MWCO PES cassette (GE healthcare) and then purified by standard chromatography on an anti-ps20 MAB, 1G7 immunoaffinity column. CM was clarified/concentrated and absorbed to an anti-ps20 (1G7) coupled NHS activated sepharose column in 25 mM Tris HCl/150 mM NaCl (pH 7.2) at a flow rate of 1 ml/min. Washing was with 5 column volumes of binding buffer and elution of ps20 was with 0.2 M glycine buffer (pH 2.3). Eluate was neutralised immediately with 1 M Tris pH 9 and dialysed overnight against PBS and aliquots stored at −80 °C. ps20 concentration was determined using a ps20 ELISA assay described in section below.

2.4.2. $rps20^{293F}$

To generate sufficient recombinant ps20 (rps20) for functional studies, we used 293 F cells, a suspension adapted cell line derived from 293T cells. An untagged ps20 construct (pBK-WFDC1) generated in Dr D Rowley's laboratory (kind gift) by cloning WFDC1 from prostate stromal cells were transfected into 293F cells using

lipofectamine (Life Technologies) and cultured in 20 × 30 ml volume FreeStyle™ 293 expression medium in conical flasks for 72 h. ps20 was purified from CM on an 1G7 affinity column, as described in Section 2.4.1 above.

2.4.3. $rps20^{FL}$, $rps20^{TR}$

In addition, smaller quantities of $rps20^{FL}$ and $rps20^{TR}$ were generated by cloning WFDC1 from HeLa cells (described in preceding section) and transfecting these constructs into adherent 293T cells followed by purification of the crude CM containing the soluble protein on 1G7 immunoaffinity column exactly as described above for $rps20^{293F}$. These preparations were used for select biochemical characterisation studies.

2.4.4. $rps20^{V5}$

Full length WFDC1 isolated from HeLa cells was cloned into a drosophila expression vector with a V5 and His tag ($rps20^{V5}$). Drosophila SH2 cells were used for protein expression and purification was by nickel-chelate as previously described [5]. Other studies (not shown) revealed that a C-terminal tag impacted biological function; therefore, $rps20^{V5}$ was used only for biochemical characterisation.

2.5. MTS viability assay

PC-3, or WPMY-1 cells seeded at 2000/well in 96 wells plates were cultured in the indicated conditions for 72 h followed by addition of 15 µl of Celltiter® reagent for 1 h. Colourimetric reading was taken by measuring absorbance at 490 nm using a plate reader (Biorad).

2.6. ps20 ELISA

96-well plates (NUNC, Thermo Fischer Scientific, USA) were coated with anti-ps20 rabbit-polyclonal antibody (5301 or 651) at 8 µg/ml overnight and blocked with 200 µl PBS with 1% Bovine serum albumin (BSA) (Sigma Aldirch) (w/v) for 2 h at room temperature (RT). 100 µl of samples or CM were incubated for 2 h at RT. An 8 point standard curve was prepared using serial 2 fold dilutions of ps20-GST fusion protein in PBS purchased from Proteintech (Manchester, UK) starting at 50ng/ml. Washing was with PBS with 0.2% Tween20 (v/v). Detection was with 1G7 conjugated to HRP at 3.7 µg/ml in PBS with 1% BSA (w/v) and 0.4%Tween20 (v/v)(Sigma Aldrich) for 2 h, and developed with 150 µl of substrate buffer (Sigma fast OPD, Sigma Aldrich) and stopped at 30 min by addition of 25 µl 4 M H_2SO_4. Absorbance at 490 nm was measured using a colorimetric plate reader (Biorad). The unknown concentrations of ps20 in samples were determined relative to the ps20-GST standard by 4 parameter logistic nonlinear regression using prism 4 (Graphpad).

2.7. SDS-PAGE/western blotting

Samples were prepared in NuPage™ LDS loading buffer and reducing reagent, boiled for 5 min and electrophoresed on 12% NuPage Bis-Tris gels (all Invitrogen Life Technologies). Gels were stained with Lumitein stain (Biotium, CA, USA) or silver stain (Sigma) according to manufacturer's instructions and visualised using a typhoon fluorescent scanner (GE Healthcare), or protein was transferred to nitrocellulose membranes and blocked using PBS with 5% milk (w/v) and 0.2% Tween20 (v/v). Hybridisation was overnight at 4 °C with anti-ps20 primary antibodies at 1:500 dilution and secondary anti-rabbit at 1:2000 dilution, simultaneously. Washing was with 10 ml PBS with 0.2% Tween20 (v/v) at room temperature 6 times for 10 min followed by incubation with ECL substrate (Thermo scientific) and acquisition using the Imagequant™ system (GE Healthcare).

2.8. Glycosaminoglycan binding studies

Using an Aktä-purifier FPLC system (GE Healthcare). 5 ml of 293T-ps20 CM was absorbed to a 1 ml HiTrap™ heparin-coated column (GE Healthcare) followed by 5 CV of washing with 50 mM Tris–HCl buffer (pH 7.5). A 0–0.5 M NaCl gradient was then applied to the column over 10 CV while 0.5 ml fractions were collected. These were then subjected to WB with 1G7. Heparin binding plates (BD Biosciences) coated overnight with 25 µg/ml GAGs; heparin sulphate, chondroitin sulphate A, and chondroitin sulphate C (all Sigma Aldrich) and blocked in PBS with 1% BSA (w/v). rps^{20293F} diluted in PBS was absorbed for 2 h prior to washing and detection with 1G7-HRP. 100 µl of tetramethylbenzidine ELISA substrate was added and absorbance at 450 nm was measured as described for the ps20 ELISA above. A baseline was established by binding of $rps20^{293F}$ to a BSA solid phase. For the cell binding assay 293T cells, pre-treated with sodium chlorate where indicated, were resuspended using PBS (Gibco) with 4 mM EDTA (Sigma Aldrich). 10^6 cells were incubated with $rps20^{V5}$ +/− heparin with agitation for 1 h. Cells were washed once with 1 ml PBS and resuspended in 50 µl tissue lysis buffer (Sigma). Samples were then subjected to WB as indicated.

2.9. Transglutaminase studies

Tissue transglutaminase (TG2) from guinea pig liver (Sigma Aldrich), was added at a final concentration of 0.1 U/ml to samples containing ps20 with 4 mM DTT and 10 mM $CaCl_2$ and incubated between 5 min and 3 h at 37ºC. Transglutamination was stopped by adding WB loading buffer and samples were boiled and analysed by WB. A modified ELISA used nunc 96 well plates coated overnight with fibronectin (Sigma) at 1 µg/ml in PBS with 1% BSA (w/v). 80 µl of TG2 (0.1 U/ml) in 50 mM TRIS buffer with 10 mM $CaCl_2$ and 4 mM DTT (pH 7.5) were added to wells and 20 µl of ps20 was added for 2 h at 37 °C. Detection was with 1G7 conjugated to HRP at 3.7 µg/ml in PBS with 1% BSA (w/v) and 0.4% Tween20 (v/v)(Sigma Aldrich) for 2 h, and developed with 150 µl of substrate buffer (Sigma fast OPD, Sigma Aldrich) and stopped at 30 min by addition of 25 µl 4 M H_2SO_4. Absorbance at 490 nm was measured using a colorimetric plate reader (Biorad).

2.10. Cathepsin cleavage studies

Cathepsin L (CL) or cathepsin B (R&D systems) were incubated with a molar excess of ps20 in 50 mM MES buffer with 4 mM DTT (pH 5.5) for 1 h at 37 °C +/− inhibitors E-64c or E-64d (Sigma). Reactions were stopped by addition of WB loading buffer and samples were analysed as described. For the modified ELISA assay; following ps20 crosslinking to fibronectin by TG as described above, CL was prepared in 50 mM MES with 4 mM DTT (pH 5.5) and added to ELISA plates for 2 h at 37 °C. Washing and detection were as described above.

2.11. Statistical tests

Tumour cell proliferation was evaluated with an unpaired *t* test. Statistical analysis was performed with Prism version 4 (GraphPad Software, San Diego, CA). Error bars represent SE, and $P < 0.05$ was considered statistically significant.

3. Results

3.1. ps20 enrichment through interaction with glycosaminoglycans

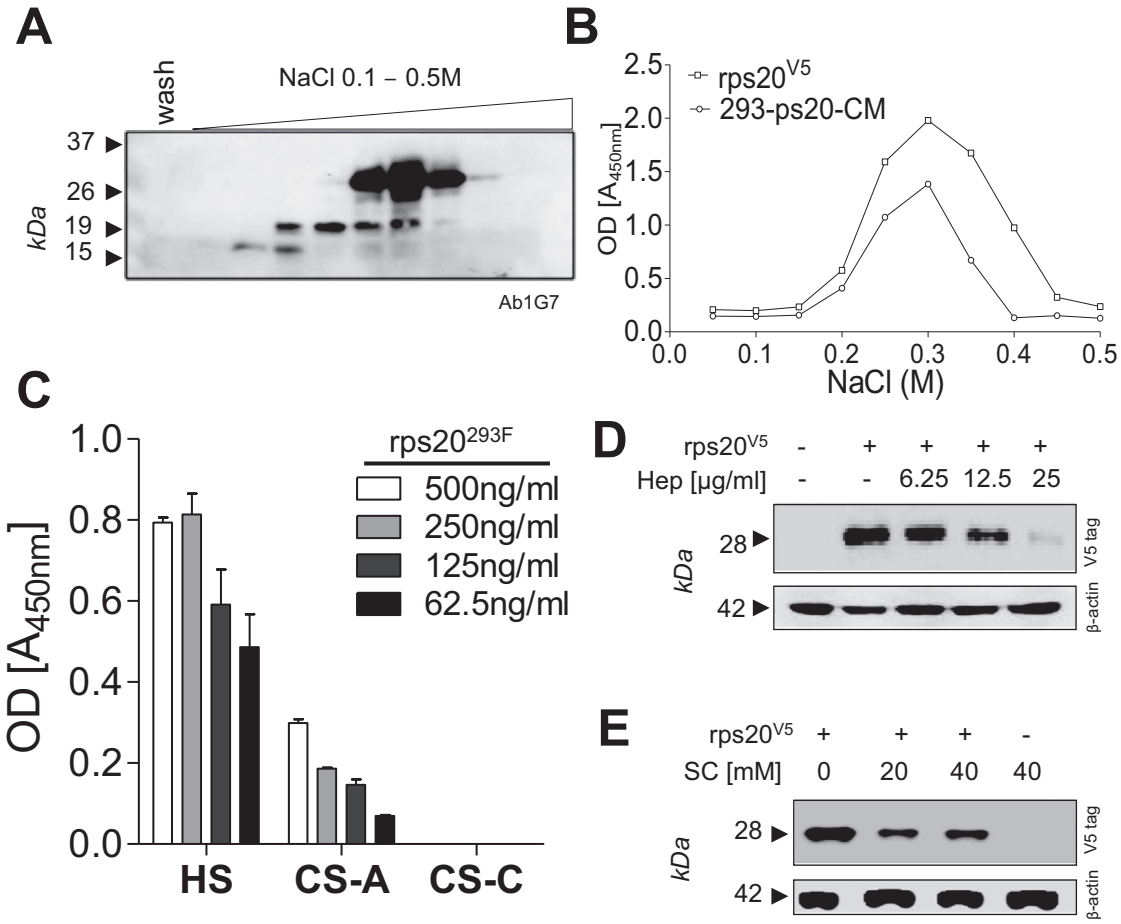

Fig. 1. ps20 enrichment through interaction with GAGs reveals multiple molecular species. (A) 5 ml of rps20-transfected 293T CM was absorbed to a heparin-sepharose column and eluted with 0–0.5 M NaCl gradient. Fractions were subjected to WB with ab1G7 under reducing conditions. (B) 5 ml of rps20-transfected 293T CM or 1 ml of a 50 ng/ml solution of $rps20^{V5}$ was absorbed to a heparin-sepharose column and eluted with 0–0.5 M NaCl gradient. Individual fractions were assayed for ps20 by ELISA. (C) $rps20^{293F}$ at the indicated concentration was bound to GAG (or BSA) coated wells for 2 h and detected using anti-V5-HRP. Baseline binding to BSA for each concentration of $rps20^{293F}$ was subtract. Charts show specific ODs; mean and SEM of two experiments in duplicate. (D–E) $ps20^{v5}$ µg/ml was absorbed to 293T cells (10^6 in presence or absence of heparin (D) or to cells treated with sodium chlorate (E). Cell were washed, lysed and subjected to WB under reducing conditions.

(GAGs) reveals multiple molecular species

We predicted that ps20 would bind GAGs based on known interactions of family members [27] and explored using this interaction to initially isolate and characterise the protein. To investigate the interaction between ps20 and GAGs we initially used crude conditioned media (CM) from 293T cells transfected to express ps20. CM was directly absorbed to and eluted from a heparin-sepharose column using a NaCl gradient (Fig. 1(A)). Notably, the concentrated 0.5 ml fractions eluted by addition of increasing concentrations of NaCl revealed for the first time numerous ps20 protein species of different molecular weights (MW) ranging from 27 kDa to 15 kDa. Fig. 1(B) shows the elution profile of ps20 using an ELISA to detect ps20 in the eluted fractions. The majority of bound ps20 was clearly eluted between 0.25 and 0.35 M NaCl. We then investigated the interaction between ps20 and physiologically relevant GAGs. Unlike heparin, heparan-sulphate and chondroitin-sulphate are expressed on the surface of cells and in the extracellular matrix (ECM) and have been shown to have important functions in the regulation of surface signalling and protein trafficking. Interestingly, rps^{20293F} had notably higher affinity for heparin-sulphate than chondroitin-sulphate-A, while no specific binding to chondroitin-sulphate-C was observed at the concentrations tested. Next, to explore if ps20 can interact with cell associated GAGs we used a purified C-terminal tagged recombinant ps20 ($rps20^{V5}$) probed with an antibody to the V5 tag. Notably, this tagged $rps20^{V5}$ had a similar elution profile to untagged ps20 when absorbed and eluted using heparin-sepharose (Fig. 1(B)). 293T cells were treated with $rps20^{V5}$ in the presence of absence of soluble heparin. Western blot analysis with anti-V5 Ab confirmed cellular $rps20^{V5}$ retention, which was interrupted in a concentration dependent manner by heparin (Fig. 1(D)). Furthermore, treatment of cells with sodium chlorate to abrogate surface glycosylation prior to treatment with $rps20^{V5}$ reduced this interaction (Fig. 1(E)). Together these data show that ps20 interacts with heparin and physiologically relevant GAGs, and can bind to cells through interactions with GAGs.

3.2. *Immunoaffinity purification enables isolation of full length and low molecular weight forms of ps20 with growth inhibitory biological activity*

To confirm the presence of multiple ps20 molecular forms, we used standard anti-ps20 Ab immunoaffinity column chromatography to generate ps20 fractions suitable for downstream biological and biochemical analysis. CM of 293F cells transfected to express pBK-WFDC1 plasmid DNA (Fig. 2(A)) was purified on anti-ps20, 1G7 MAb column. This ps20 preparation was named rps^{20293F}. Mass spec analysis revealed one significant contaminant in this material which was galectin-3 binding protein (G3BP). Western blotting with affinity purified anti-ps20 antibodies revealed one predominant molecular species of ps20 at $\approx$ 27 kDa,

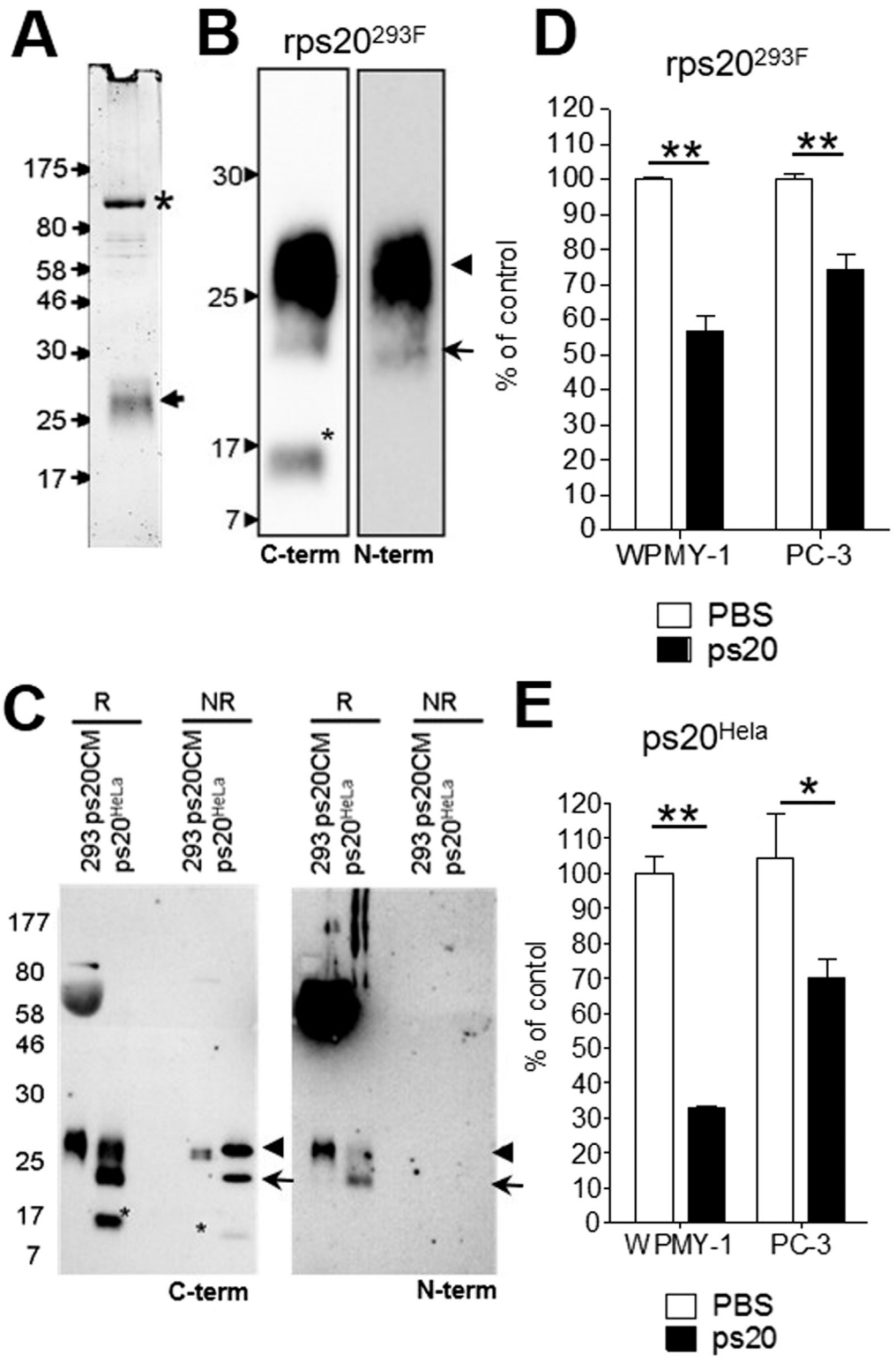

Fig. 2. Purification of functionally active ps20 using anti-ps20 immunaffinity. (A–B) Purified rps20^{293F} was subjected to SDS-PAGE followed by silver staining (A) or WB with antibodies to C- or N-terminal epitopes (B). (C) ps20^{HeLa} is shown alongside CM from 293T cells expressing pBK-WFDC1 plasmid as a positive control. The CM contained 10% FCS and there is a large amount of non-specific immunoreactivity to serum components at 60–70 kDa. Samples were electrophoresed under reducing (R) or non-reducing (NR) conditions to distinguish monomeric from multimeric protein structures. Arrowheads indicate the ps20 FL species, arrows the ps20 TR species, and LMW species are indicated with asterisks. (D) PC-3, or WPMY-1 cells were treated with rps20^{293F} (8.3 nM) and growth assessed by MTS at 72 h. (E) PC-3, or WPMY-1 cells were treated with 68pM ps20^{HeLa} (68 pM) and growth assessed by MTS at 72 h. (D and E) Mean and SEM of 3 experiments performed in duplicate. $^{*}P < 0.05$, $^{**}P < 0.001$ *by students T test*.

and confirmed several minor subspecies resolving at lower MW of 22 kDa and 15 kDa (Fig. 2(B)). The concentration of rps20^{293F} is shown in Table 1. Next, to investigate if multiple molecular forms of ps20 are natively expressed, 1G7 immunoaffinity column was again used to purify ps20 from a suspension culture of human HeLa cells (henceforth ps20^{HeLa}), which we have previously

Table 1
Immunaffinity purified batches of ps20 used in this study.

ps20 batch	Concentration (from ps20 ELISA)	Molar concentration (based on MW of 24 kDa) (nM)
$rps20^{293F}$	2 μg/ml	83
$ps20^{HeLa}$	15 ng/ml	0.68
$rps20^{FL}$	190 ng/ml	7.9
$rps20^{TR}$	184 ng/ml	7.64

reported to spontaneously secrete high levels of ps20 (Fig. 2(C)) [5].

Both the 293F- and HeLa-derived ps20 preparations $rps20^{293F}$ and $ps20^{HeLa}$ respectively) were characterised using anti-ps20 antibodies specific to N- and C-terminal regions. These experiments revealed that the ~27 kDa protein in both preparations was recognised by both the C- and N-terminal antibodies (Fig. 2(B) and (C) arrowheads). The second ~22 kDA protein was also recognised by both these antibodies and based on MW is likely the truncated form of ps20 encoded by an mRNA lacking exon 3, as previously reported (Fig. 2(B) and (C) arrows, and Supplementary Fig. 1) [13]. The third minor band at ≈15 kDa, is only detected by the C-terminal antibody in both $rps20^{293F}$ and $ps20^{HeLa}$ preparations (Fig. 2(B) and (C) asterisks), suggesting that this is a product of proteolytic cleavage close to the N-terminus of the molecule.

Previous studies have shown ps20 to display growth inhibitory effects on prostate stromal cells (6). Therefore immunoaffinity purified $rps20^{293F}$ and the $ps20^{HeLa}$ were added to PC-3 and WPMY-1 cells at a concentration comparable with that observed in previous studies [28]. The $rps20^{293F}$ preparation inhibited both PC-3 and WPMY-1 by 50% and 30% respectively (Fig. 2(D)). Likewise, $ps20^{HeLa}$ also induced potent growth inhibition on these cells (Fig. 2(E)), however, notably $ps20^{HeLa}$ was effective at a concentration 2 logs below those observed with $rps20^{293F}$ (Fig. 2(D) and (E) and Table 1) or reported previously [28]. These experiments suggest that i) ps20 is cleaved into LMW species that lack the N-terminus, and that ii) ps20 preparations that contain these forms are functionally active.

3.3. Cathepsin L cleaves ps20 at C-terminus with no impact on ps20 growth inhibitory function

We predicted that the lower MW minor forms of ps20 present in $rps20^{293F}$ and $ps20^{HeLa}$ (Fig. 2(B) and (C)) preparations may arise by proteolytic cleavage by cathepsins or other extracellular proteases, based on similar characteristics of other WAP proteins [26,29]. This was formally tested first using sequence verified rps20 preparations that lacked the minor lower MW forms: namely, $rps20^{FL}$, and the exon 3 truncated $rps20^{TR}$ (generated as described in materials and methods, the concentrations of ps20 preparations are shown in Table 1). These samples each resolved as a single ps20 band at the expected size of 27 kDa and 22 kDa respectively (Fig. 3(A) and (B) right panel).. These purified $rps20^{FL}$ and $rps20^{TR}$ preparations were then subjected to proteolytic cleavage. Numerous proteases tested including furin, thrombin, various matrix metalloproteases (not shown) and cathepsin-B (CB) (Fig. 3(A)) failed to cleave ps20. However, when incubated with cathepsin-L (CL) a 4–6 kDa cleavage of both $rps20^{FL}$ and $rps20^{TR}$ was clearly evident when probed with the N-terminal specific anti-ps20 antibody (Fig. 3(B), upper panels). In contrast, when probed with the C-terminal anti-ps20 antibody (Fig. 3(B), lower panels), we observed the disappearance of ps20, highlighting a specific CL cleavage near the C-terminus.

Addition of CL inhibitors (E64c and E64d) to a CL-$rps20^{FL}$ cleavage reaction inhibited this process highlighting the specificity of CL cleavage (Fig. 3(C)). On the other hand heparin did not enhance or inhibit this cleavage, further highlighting CL cleavage specificity (Fig. 3(C)). To determine if ps20 cleavage by CL impacted biologically activity, we added CL to $rps20^{293F}$ (Fig. 3(D) and (E) lower panel). This revealed a clear shift of electrophoretic mobility of ps20 bands (Fig. 3(D), arrows), resulting in a number of further LMW ps20 species (≈10 kDa, 15 kDa), suggesting CL was able to cleave ps20 species with an intact C-terminus. To test impact on biological activity, CL cleaved $rps20^{293F}$ was added to WPMY-1 prostate cells. CL cleavage resulted in no change to $rps20^{293F}$ growth inhibitory function (Fig. 3(E)).

Taken together, these experiments indicate that CL cleaves ps20 at the C terminus to generate minor lower MW ps20 species, and does not abrogate ps20 growth inhibitory function.

3.4. CL mediated cleavage is important for ps20 cross-linking to fibronectin by transglutaminase

As CL cleavage did not abrogate the growth inhibitory activity of ps20, we tested its importance in a second function that WAP proteins are implicated in: that is cross-linking to the ECM via transglutaminase (TG2) [24,25]. The interaction between ps20 and solid phase TG2 was first tested using $rps20^{V5}$ in a modified ELISA, which confirmed a high-level of binding of ps20 to TG2 relative to a BSA solid phase (not shown).

We then assessed the ability of TG2 to catalyse the formation of ps20 into high MW (HMW) forms using $rps20^{293F}$. Fig. 4(A), right panel, shows a TG2 dependent multimerisation of rps^{20293F} to a predominant ≈150 kDa species, and a less distinct HMW species, which failed to migrate into the gel, suggesting that TG2 induces the formation of higher order multimers of ≈150 kDa and above. Interestingly, the same experiment WB using a ps20 C-terminal antibody (Fig. 4(A), left panel) shows only the monomeric protein, which is absent following incubation with TG, but fails to reveal the multimerised forms, implying the involvement of the C-terminal glutamine residues in the transglutaminase reaction, which would block binding of our C-terminal antibody. To further verify that this finding was the result of a TG2 mediated transamidation reaction we incubated $rps20^{V5}$, which can be visualised by probing the c-terminal V5 tag, with TG2 for the indicated time, or in the presence of EDTA, or competitive TG2 inhibitor cystamine (Fig. 4(B)). TG2 catalysed the formation of a multimeric ≈150 kDa ps20 species, and a continuum of higher order ps20 species >150 kDa. Conversely, the presence of chelating agent EDTA, or cystamine prevented the formation of any such multimerisation, providing a strong indication that TG2 induced transamidation was the cause of ps20 multimerization.

We then investigated the interaction between ps20 and fibronectin, a component of the ECM with which SLPI and elafin have also been shown to functionally interact and become cross-linked to [24,25]. TG2 efficiently catalysed cross-linking of $rps20^{293F}$ to fibronectin in a modified ELISA assay; only a small level of binding to fibronectin was observed in the absence of TG2, or the presence of EDTA, suggesting that *bona fide* TG2 dependent cross-linking of ps20-fibronectin was occurring (Fig. 4(B)). In contrast, no significant interaction was seen between ps20 and BSA either in the presence or absence of TG2, suggesting the crosslinking between fibronectin and ps20 catalysed by TG2 was a specific interaction. In order to assess whether the CL cleavage impacted this function, we performed a digestion of $rps20^{293F}$ with CL, followed by incubation with TG2 to mediate the formation of HMW multimers (Fig. 4(C)). Multimerisation is far less apparent in $rps20^{293F}$ which has been cleaved by CL, again suggesting that TG2 mediated cross-linking involves the C-terminus of ps20 which has 3 glutamine residues within the last 10 aa, which is the predicted cleavage site of CL. We then tested if ps20 immobilised and bound to fibronectin could be cleaved by CL

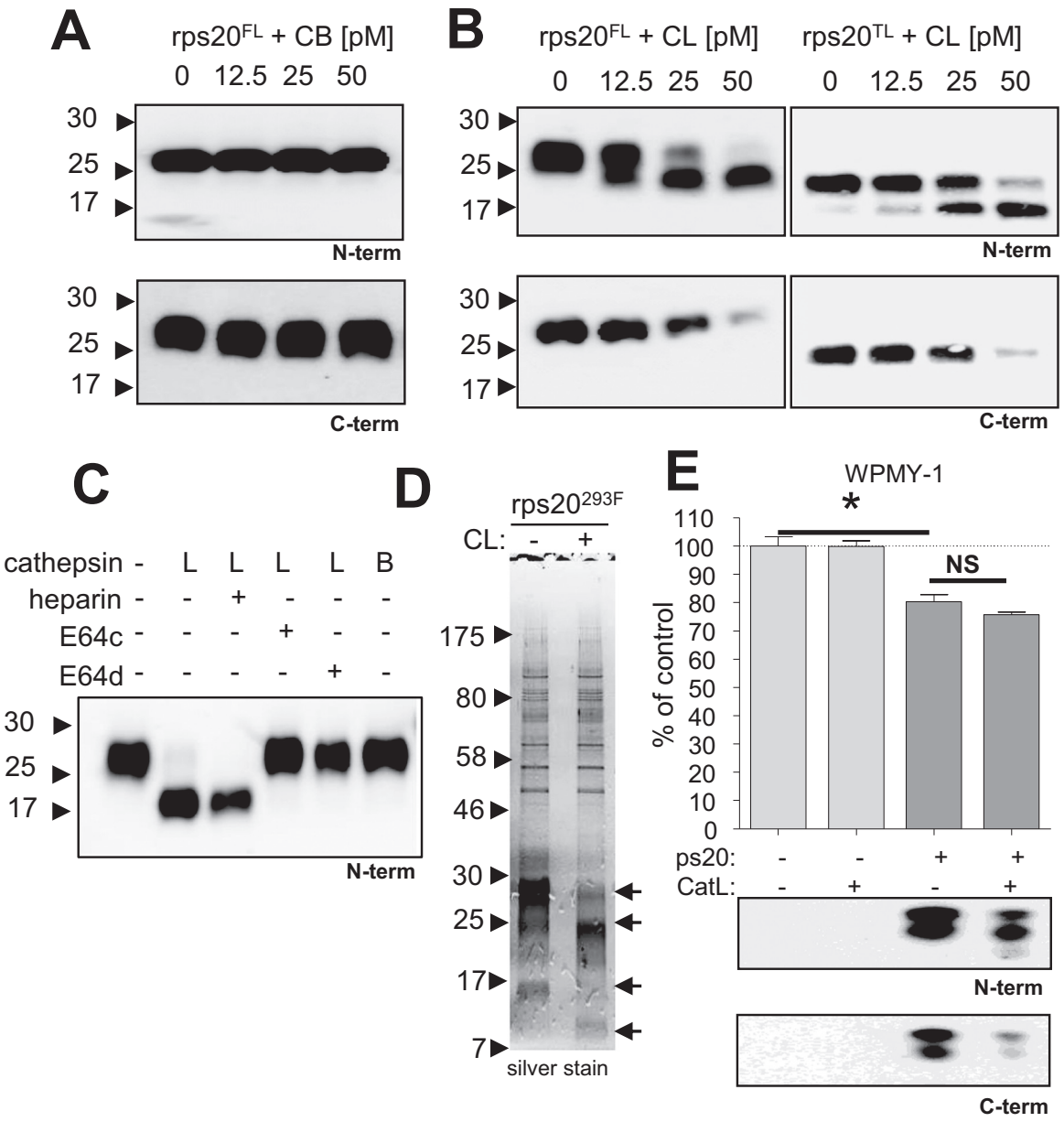

Fig. 3. rps20^{FL} and rps20^{TR} are cleaved at the C-terminus by CL. (A) rps20^{FL} (100 ng/ml/1.8 nM) was incubated with an increasing concentration of CB followed by WB. (B) rps20^{FL} or rps20^{TR} (both 100 ng/ml/1.8 nM) was cleaved by CL at the indicated concentration and subjected to WB. (C) rps20^{FL} (100 ng/ml/1.8 nM) was incubated with CL (50 pM) in the presence of absence of inhibitors (30 μM), or with CB (50 pM) and subjected to WB. (D) rps20^{293F} 1 ug/ml, was incubated with 200 ng/ml CL before SDS-PAGE analysis under reducing conditions. (E) 10 μl of each reaction from C was added to WPMY-1 cells (Final concentration 4.15 nM). Proliferation was assessed at 72 h by addition of MTS reagent (Mean and SEM of two experiments in duplicate). Alternatively samples were subjected to WB under reducing conditions (D, lower panel). *$p < 0.05$ *by students T test.*

resulting in release of soluble ps20 and accumulation of the N-terminal portion of the molecule in solution (Fig. 4(D)). As before, we observed high levels of ps20 cross-linked to fibronectin in the presence of TG2, but far lower with either solid phase BSA or where TG2 was absent (Fig. 4(D)). Following the crosslinking step, the plate was washed and incubated with CL, which reduced the ps20 bound to fibronectin almost to baseline levels. This demonstrates that even after ps20 is cross-linked to fibronectin via TG2, it is susceptible to CL-mediated cleavage at the C-terminus.

Taken together these data show that ps20 interacts with TG2 and undergoes multimerisation and cross-linking to the ECM protein fibronectin. Furthermore, once cross-linked to fibronectin, CL can continue to cleave ps20 at the C-terminus.

4. Discussion

Despite evidence of significant functional relevance to cancer, cell senescence, and the outcome of viral infections, ps20 remains largely uncharacterised at the protein level. We demonstrate that ps20 is a GAG binding factor like SLPI and elafin [15,16], capable of interactions with heparin and physiological GAGs heparan-sulfate and chondroitin sulphate. Furthermore, ps20-interactions binding to cells was outcompeted by heparin, suggesting an interaction with cell surface glycosaminoglycans. Given the current lack of understanding about the mechanisms of ps20 and other WFDC protein function, this attribute may have important functional implications. Notably, SLPI function is mediated by the ability to

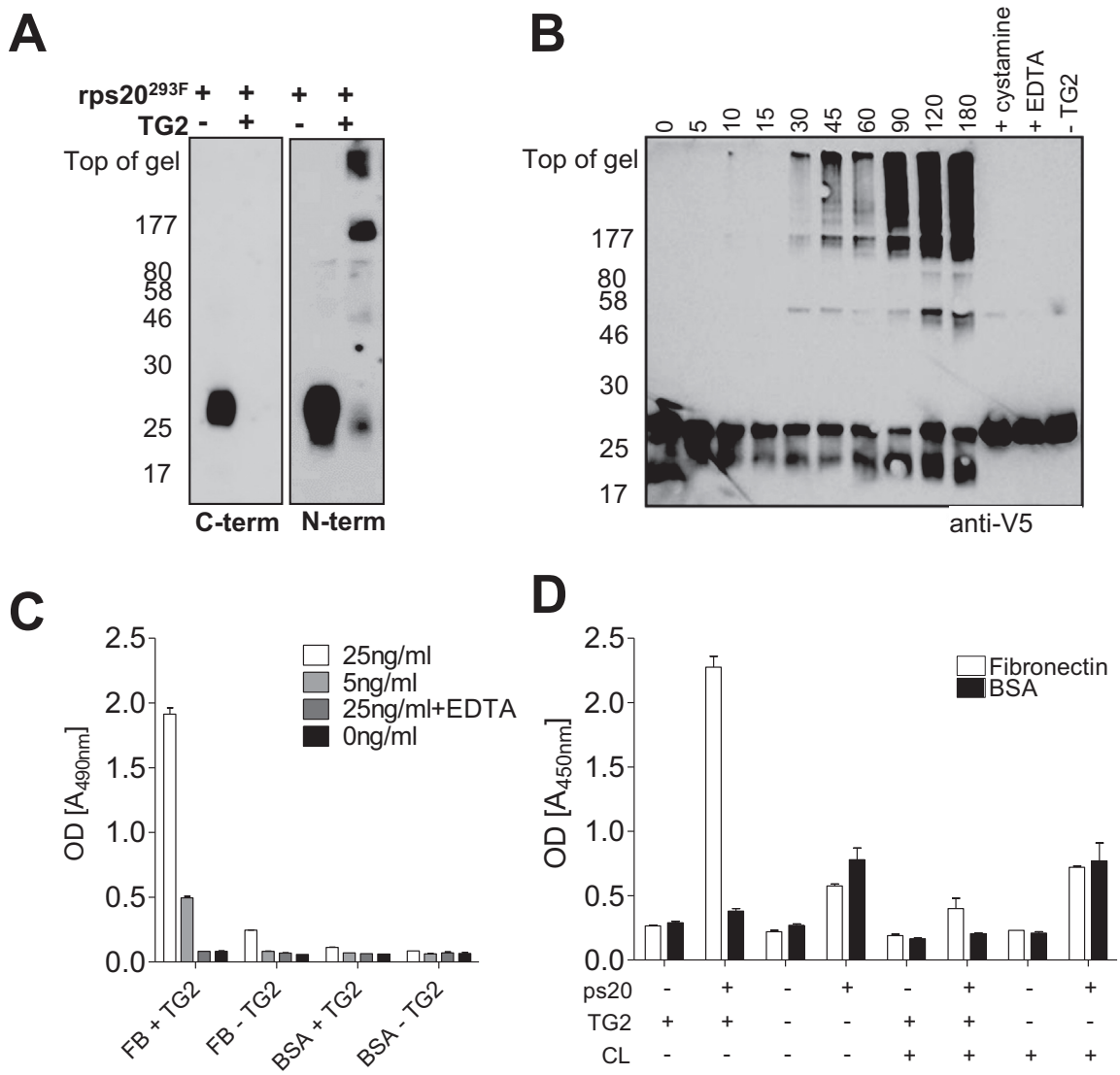

Fig. 4. ps20 undergoes transglutaminase dependent crosslinking to fibronectin. (A) rps20^{293F} was incubated with TG2 or buffer control for 1 h followed WB with the indicated antibodies. (B) rps20^{V5} was incubated with TG2 for the indicated time, or with the inhibitor indicated for 3 h. Samples were subjected to WB with anti-V5. All samples were blotted under reducing conditions. (C) rps20^{FL} at the indicated concentration was incubated with/without TG2 and/or EDTA in an ELISA plate coated with BSA or fibronectin. ps20 detection was with 1G7-HRP. (D) rps20^{FL} was crosslinked to fibronectin as described for (C), after washing, well were incubated +/− CL (50 pM). ps20 detection was with 1G7-HRP. (C and D, means and SEM of duplicate and triplicate wells respectively).

cross the membrane and interact intracellularly [21,22]. Evidence from studies with cationic peptides such as HIV-TAT indicates that surface-proteoglycans can mediate macropinocytotic protein/peptide uptake [30,31]. Future work with ps20 and other WFDC family proteins should therefore consider protein-GAG interactions as a potential mechanism of cellular signalling.

To date, functional investigation of ps20 has been limited by the available sources of the protein. C-terminal GST tagged protein is available commercially, although this tag has previously been shown to interfere with the growth suppression activity [6]. In addition, we have failed to observe any function in V5-His tagged ps20, suggesting that C-terminal tags may be broadly inhibitory to ps20 function. Furthermore, crude CM from cells transfected to express rps20 has repeatedly failed to inhibit cellular proliferation, despite achieving high concentrations [13]. We utilised immunoaffinity chromatography with anti-ps20 1G7 to purify recombinant ps20 from 293F cells (rps20^{293F}, Fig. 2(A)) as well as native ps20 secreted by HeLa cells (ps20^{HeLa}, Fig. 2(C)). In line with previously published reports [6,28] rps20^{293F}, which contained multiple LMW forms (≈ 22 kDa, ≈ 15 kDa), inhibited growth of prostate cancer cells (Fig. 2(C)) at low nanomolar concentration, while the sole contaminant G3BP showed no growth inhibitory function at micromolar concentrations (not shown). Purification of native ps20 from HeLa CM also revealed multiple LMW anti-ps20 immuno-reactive protein species resolving at ≈ 22 kDa and ≈ 15 kDa, and was similarly biologically active in cell growth inhibition assays (Fig. 2(E)). Notably, WB of ps20 preparations including rps20^{293F} and ps20^{HeLa} with anti-ps20 Ab to both C-and N-terminal regions revealed the presence of the protein product of an exon 3 truncated WFDC1 mRNA described [6] and previously cloned and expressed by our lab [13].

The presence of a prominent cleaved subspecies resolving at ≈ 15 kDa in the ps20^{HeLa} lacking the ps20 N-terminal epitope, combined with its potent growth inhibitory activity at concentrations 2 logs below rps20^{293F} led us to postulate that LMW ps20 species may be functionally important. To test this possibility we subjected ps20 preparations to protease cleavage. While thrombin, furin, metalloproteinase-3 and cathepsin-B failed to cleave ps20, we showed that CL can efficiently cleave all ps20 preparations tested at the C-terminus at concentrations far below

that reported for CL physiological activity [32] (Fig. 3(B)). However, this resulted in neither enhancement, nor abrogation of $rps20^{293F}$ mediated growth inhibition (Fig. 3(E)) suggesting CL cleavage is not a regulator of ps20's growth inhibitory activity. Furthermore, the use of specific CL inhibitors, and the fact that cathepsin B and other proteases had no effect of ps20 suggests that he CL cleavage reaction is specific and may have relevance aside from the generation of growth inhibitory ps20 cleavage products.

To further investigate the putative biological significance of CL-mediated cleavage of ps20, we explored its impact on a second known function of WAP proteins, that of binding / cross-linking to the ECM. First we tested if ps20 interacts with transglutaminase2 (TG2). We observed high-affinity binding of ps20 to a TG2 solid-phase (not shown). TG2 is best known for its ability to cross-link proteins via a transamination reaction. In line with this we observed the TG2 dependent formation of 150 kDa and higher ps20 multimers (Fig. 4) indicating that TG2 regulates the multimerisation of ps20 into non-labile multimers resistant to reduction by boiling in DTT. Interestingly, untagged ps20 multimers were only detected by anti-ps20 directed against the N-terminus of the protein, suggesting ps20 cross-linking involves one or more of the three glutamines in the immediate C-terminal region of ps20. Next, and in line with similar studies demonstrating that SLPI and elafin can cross-link with fibronectin [24,25], we show here that ps20 can also become cross-linked to fibronectin in a TG2 dependent fashion. Given the suspected involvement of the C-terminus in ps20 cross-linking, we then tested the impact of CL cleavage of ps20 following TG2-mediated ps20 cross-linking to fibronectin (Fig. 4(D)). Following TG2 mediated cross-linking of ps20 to fibronectin, the failure to detect ps20 in those conditions subjected to subsequent CL cleavage (Fig. 4(D)) suggests a possible mechanism for the release of soluble ps20 from the ECM matrix through C-terminal cleavage. It remains possible, however, that the failure to detect ps20 cross-linked to fibronectin, following cleavage by CL may instead be due to changes to fibronectin solid phase induced by CL. However, the ultimate effect of liberating ps20 from the interaction appears to be the same. Lastly, while it is clear then that CL can cleave ps20 at the C-terminus, and this may play a role in regulating interactions with ECM components, it is possible that CL cleavage of ps20 may also have as yet unidentified functions. In light of the numerous indications that ps20 possesses pleiotropic functionality [3–5,9,13,33], it may be the case that CL and possibly other proteases regulate the function of ps20 through tissue and cell-type specific cleavage events by i) generating functional protein fragments, or ii) abrogating interactions with other tissue components, such as fibronectin.

Our demonstration that ps20 interacts with GAGs may be pertinent in light of recent data suggesting TG2 function is regulated at the cell surface through interactions with GAGs. While we saw no enhanced TG2-dependent multimerization of ps20 in the presence of soluble heparin (not shown), it may be the case that within tissues - at the ECM or cell surface - the interaction of ps20, TG2 [34,35], and CL [36] with surface GAGs regulates the processes observed herein. We propose that ps20 is secreted by cells in both FL and TR forms and cleaved into smaller variants by as yet unidentified proteases. Interactions with GAGs, TG2 and cathepsins then comprise an apparatus, common to SLPI, elafin and ps20, whereby bioavailability of ps20 is regulated through the formation of HMW multimers, or through cross-linking to the ECM, and in-turn liberated by CL or similar proteolytic cleavage. Using in vitro assays, we have demonstrated that ps20 has numerous biochemical properties in common with other WFDC family proteins that will be important to consider in further investigating the function of this molecule.

It is noteworthy, that despite dozens of publications describing diverse functional activities of WFDC family proteins, no receptors have been identified for any family member. We suggest that due to the possibly unique properties of this protein family, the standard secreted-protein interaction with cognate-receptor paradigm of signalling may not be relevant. For WFDC family proteins there is increasing evidence that extracellular processing events are necessary to generate protein fragments which may have diverse signalling modalities. Some of these functions may involve cognate receptors, though none have yet been identified, or they may involve crossing the cell-membrane and interacting with cellular components, or DNA directly, as has been observed for SLPI [21]. WFDC proteins, including ps20, should therefore be studied further to elucidate their biochemical complexity, as they may function through interesting and as yet unidentified mechanisms, broadly relevant to our understanding of cell biology.

Acknowledgement

This work was partly funded by a Heathside Charitable Trust grant to PD, an International Consortium for Novel Antiviral Grant to AV. OJH, CG, AV, and RAS conceived the project, OJH performed the experimental work. We thank Sangmi Kim for assistance with initial ELISA and WB protocols.

Appendix A. Transparency document

Transparency document associated with this article can be found in the online version at 10.1016/j.bbrep.2016.06.010.

Appendix B. Supplementary material

Supplementary material associated with this article can be found in the online version at 10.1016/j.bbrep.2016.06.010i.

References

[1] M. Tsunemi, et al., Crystal structure of an elastase-specific inhibitor elafin complexed with porcine pancreatic elastase determined at 1.9 A resolution, Biochemistry 35 (36) (1996) 11570–11576.
[2] C.D. Bingle, A. Vyakarnam, Novel innate immune functions of the whey acidic protein family, Trends Immunol. 29 (9) (2008) 444–453.
[3] S.J. Ressler, et al., WFDC1 is a key modulator of inflammatory and wound repair responses, Am. J. Pathol. (2014).
[4] E. Rogers, et al., WFDC1/ps20: a host factor that influences the neutrophil response to murine hepatitis virus (MHV) 1 infection, Antivir. Res. 96 (2) (2012) 158–168.
[5] R. Alvarez, et al., WFDC1/ps20 is a novel innate immunomodulatory signature protein of human immunodeficiency virus (HIV)-permissive CD4+ CD45RO+ memory T cells that promotes infection by upregulating CD54 integrin expression and is elevated in HIV type 1 infection, J. Virol. 82 (1) (2008) 471–486.
[6] M. Larsen, et al., Molecular cloning and expression of ps20 growth inhibitor. A novel WAP-type “four-disulfide core” domain protein expressed in smooth muscle, J. Biol. Chem. 273 (8) (1998) 4574–4584.
[7] S.J. Ressler, D.R. Rowley, The WFDC1 gene: role in wound response and tissue homoeostasis, Biochem. Soc. Trans. 39 (5) (2011) 1455–1459.
[8] H. Hung, Suppression of ps20 expression in the rat uterus by tamoxifen and estrogens, Endocrinology 146 (5) (2005) 2388–2396.
[9] S. Madar, et al., Modulated expression of WFDC1 during carcinogenesis and cellular senescence, Carcinogenesis 30 (1) (2009) 20–27.
[10] S.J. McAlhany, et al., Decreased stromal expression and increased epithelial expression of WFDC1/ps20 in prostate cancer is associated with reduced recurrence-free survival, Prostate 61 (2) (2004) 182–191.
[11] J.E. Watson, et al., Molecular analysis of WFDC1/ps20 gene in prostate cancer, Prostate 61 (2) (2004) 192–199.
[12] S. Liu, et al., Expression and functional analysis of the WAP four disulfide core domain 1 gene in human melanoma, Clin. Exp. Metastasis 26 (7) (2009) 739–749.
[13] O.J. Hickman, et al., Expression of two WFDC1/ps20 isoforms in prostate stromal cells induces paracrine apoptosis through regulation of PTGS2/COX-2, Br. J. Cancer (2016).

[14] D. Guerrieri, et al., Serine leucocyte proteinase inhibitor-treated monocyte inhibits human CD4(+) lymphocyte proliferation, Immunology 133 (4) (2011) 434–441.
[15] K. Baranger, et al., The antibacterial and antifungal properties of trappin-2 (pre-elafin) do not depend on its protease inhibitory function, FEBS J. 275 (9) (2008) 2008–2020.
[16] M.A. Fath, et al., Interaction of secretory leukocyte protease inhibitor with heparin inhibits proteases involved in asthma, J. Biol. Chem. 273 (22) (1998) 13563–13569.
[17] M. Nakamura, et al., Sulfated glycosaminoglycans are required for specific and sensitive fibroblast growth factor (FGF) 19 signaling via FGF receptor 4 and betaKlotho, J. Biol. Chem. 286 (30) (2011) 26418–26423.
[18] T.M. Handel, et al., Regulation of protein function by glycosaminoglycans–as exemplified by chemokines, Annu. Rev. Biochem. 74 (2005) 385–410.
[19] S. Kobialka, et al., Glycosaminoglycan chains affect exocytic and endocytic protein traffic, Traffic 10 (12) (2009) 1845–1855.
[20] M.E. Favretto, et al., Glycosaminoglycans in the cellular uptake of drug delivery vectors – bystanders or active players? J. Control Release 180 (2014) 81–90.
[21] C.C. Taggart, et al., Secretory leucoprotease inhibitor binds to NF-kappaB binding sites in monocytes and inhibits p65 binding, J. Exp. Med. 202 (12) (2005) 1659–1668.
[22] S.S. Hannila, et al., Secretory leukocyte protease inhibitor reverses inhibition by CNS myelin, promotes regeneration in the optic nerve, and suppresses expression of the transforming growth factor-beta signaling protein Smad2, J. Neurosci. 33 (12) (2013) 5138–5151.
[23] L. Lorand, S.M. Conrad, Transglutaminases, Mol. Cell Biochem. 58 (1–2) (1984) 9–35.
[24] N. Guyot, et al., Elafin and its precursor trappin-2 still inhibit neutrophil serine proteinases when they are covalently bound to extracellular matrix proteins by tissue transglutaminase, Biochemistry 44 (47) (2005) 15610–15618.
[25] K. Baranger, et al., Secretory leukocyte protease inhibitor (SLPI) is, like its homologue trappin-2 (pre-elafin), a transglutaminase substrate, PLoS One 6 (6) (2011) e20976.
[26] J.M. Sallenave, et al., Regulation of secretory leukocyte proteinase inhibitor (SLPI) and elastase-specific inhibitor (ESI/Elafin) in Human airway epithelial cells by cytokines and neutrophilic enzymes, Am. J. Respir. Cell Mol. Biol. 11 (6) (1994) 733–741.
[27] C.C. Taggart, et al., Cathepsin B, L, and S cleave and inactivate secretory leucoprotease inhibitor, J. Biol. Chem. 276 (36) (2001) 33345–33352.
[28] D.R. Rowley, et al., Purification of a novel protein (ps20) from urogenital sinus mesenchymal cells with growth inhibitory properties in vitro, J. Biol. Chem. 270 (37) (1995) 22058–22065.
[29] S.W. Cox, et al., Secretory leukocyte protease inhibitor and its potential interactions with elastase and cathepsin B in gingival crevicular fluid and saliva from patients with chronic periodontitis, J. Periodontal Res. 41 (5) (2006) 477–485.
[30] J.M. Gump, R.K. June, S.F. Dowdy, Revised role of glycosaminoglycans in TAT protein transduction domain-mediated cellular transduction, J. Biol. Chem. 285 (2) (2010) 1500–1507.
[31] K. Lambaerts, S.A. Wilcox-Adelman, P. Zimmermann, The signaling mechanisms of syndecan heparan sulfate proteoglycans, Curr. Opin. Cell Biol. 21 (5) (2009) 662–669.
[32] S. Inayat, et al., High levels of cathepsins B, L and S in human seminal plasma and their association with prostasomes, Andrologia 44 (6) (2012) 423–427.
[33] S.J. McAlhany, et al., Promotion of angiogenesis by ps20 in the differential reactive stroma prostate cancer xenograft model, Cancer Res. 63 (18) (2003) 5859–5865.
[34] A. Scarpellini, et al., Syndecan-4 knockout leads to reduced extracellular transglutaminase-2 and protects against tubulointerstitial fibrosis, J. Am. Soc. Nephrol. 25 (5) (2014) 1013–1027.
[35] A. Scarpellini, et al., Heparan sulfate proteoglycans are receptors for the cell-surface trafficking and biological activity of transglutaminase-2, J. Biol. Chem. 284 (27) (2009) 18411–18423.
[36] K. Ishidoh, E. Kominami, Procathepsin L degrades extracellular matrix proteins in the presence of glycosaminoglycans in vitro, Biochem. Biophys. Res. Commun. 217 (2) (1995) 624–631.